A Study of the Seasonal Variations of the Chandra X-ray Observatory Radiation Model

J. M. DePasquale[a], S. N. Virani[a], D. A. Schwartz[a], R. A. Cameron[a], P. P. Plucinsky[a], S. L. O'Dell[b], J. I. Minow[c] and W. C. Blackwell, Jr[c]

[a]Harvard-Smithsonian Center for Astrophysics, 60 Garden Street, Cambridge, MA, USA
[b]NASA Marshall Space Flight Center, Huntsville, AL, USA
[c]Jacobs Sverdrup, Marshall Space Flight Center, Huntsville, AL, USA

ABSTRACT

The *Chandra* X-ray Observatory (CXO), launched in July of 1999, contains two focal-plane imaging detectors and two transmission-grating spectrometers. Maintaining an optimal performance level for the observatory is the job of the *Chandra* X-ray Center (CXC), located in Cambridge, MA. One very important aspect of the observatory's performance is the science observing efficiency. The single largest factor which reduces the observing efficiency of the observatory is the interruption of observations due to passage through the Earth's radiation belts approximately every 2 2/3 days. During radiation belt passages, observations are suspended on average for over 15 hours and the Advanced CCD Imaging Spectrometer (ACIS) is moved out of the focus of the telescope to minimize damage from low-energy (100-200 keV) protons. The CXC has been using the National Space Science Data Center's "near Earth" AE-8/AP-8 radiation belt model to predict the entry and exit from the radiation belts. However, it was discovered early in the mission that the AE-8/AP-8 model predictions were inadequate for science scheduling purposes and a 10 ks "pad time" was introduced on ingress and egress of perigee to ensure protection from radiation damage.[1] This pad time, totaling 20 ks per orbit, has recently been the subject of much analysis to determine if it can be reduced to maximize science observing efficiency. A recent analysis evaluating a possible correlation between the *Chandra* Radiation Model (CRM) and the Electron Proton Helium Instrument (EPHIN) found a *greatest lower bound* (*GLB*) in lieu of a correlation for the ingress and egress of each perigee.[2] The *GLB* is a limit imposed on the CRM such that when the CRM exceeds this limit on ingress, this defines the new safing time and similarly for egress. We have shown that using this method we can regain a significant amount of lost science time at the expense of minimal radiation exposure. The *GLB* analysis also found that different *GLB's* produce varied results and hint that there could be a time dependence associated with the *GLB*, possibly related to the orientation of the Observatory's orbit. Utilizing CRM V2.3, we present the search for a seasonal dependence on the value of the *GLB*; we find a seasonal effect that appears to depend on the orientation of *Chandra's* orbit with respect to the Earth's magnetic field.

Keywords: Chandra, space missions, radiation environment, radiation belts, radiation models

1. INTRODUCTION

As of 23 July 2003 the *Chandra* X-ray Observatory (CXO) has been in Earth orbit for 4 years. This observatory has contributed over 3700 observations to date toward the advancement of our understanding of the universe. *Chandra* has provided some of the most exquisitely sensitive X-ray observations. Maximizing the amount of time devoted towards science observations is a major concern of many of the groups involved in keeping the Observatory operational. As our models of the various space environments that *Chandra* encounters become more sophisticated and mature, we will undoubtedly regain a large portion of the useful science observing time that is currently not utilized in each orbit in order to protect the science instruments from radiation damage in the inner magnetosphere.[3] Until the models become more accurate, we rely on past experience and a wealth of

Further author information: (Send correspondence to J.M.D.)
J.M.D.: E-mail: jdepasquale@cfa.harvard.edu, Telephone: 1 617 495 7025

data that 4 years in orbit has provided. We attempt to provide a robust, predictive constraint on a maximum flux per orbit such that *Chandra* will be able to maintain a nominal observation closer to entering the radiation zone than is now possible. Likewise, upon exiting the radiation zone, this constraint will enable *Chandra* to resume nominal science operations sooner than is now possible.

2. DATA & ANALYSIS

All aspects of the *GLB* analysis depend on databases created as a filtered subset of existing databases. More specifically, there are 3 databases extensively used here including CRMFLX, which drives the CRM, the EPHIN database and a database of *Chandra* orbital events.

2.1. CRM, EPHIN & ORBITAL EVENTS DATABASES

Using FORTRAN code linked to CRM V2.3 and a *Chandra* ephemeris, a CRM flux database was created for the length of the *Chandra* mission from launch to February 2003.[4] This particular CRM database includes a conservative, fixed geomagnetic planetary activity index – KP = 3, with no solar wind component. Although *Chandra's* eccentric orbit samples a wide array of space environments including the magnetosheath, the magnetosphere and the solar wind, the solar wind component of the CRM does not contribute significantly to the flux measured in the inner magnetosphere for proton energies (0.1–0.5 MeV) most damaging to the CCDs. The inner magnetosphere is largely dominated by trapped radiation and it is the only region that *Chandra* encounters during perigee passage, which is of course the section of the orbit in which this analysis is most concerned. Thus, we do not include a solar wind component in the CRM database for this analysis. For a more in depth discussion of the CRM please refer to Virani et al., these proceedings.

The EPHIN database used in this analysis has been updated daily since launch. It contains 5 minute samples of data from all channels of EPHIN. The EPHIN channels of interest to this analysis, namely P4 (protons from 5.0 - 8.3 MeV) and E1300 (electrons from 2.64 - 6.18 MeV), were extracted from the database and written to a new database along with the time.

The command loads for each *Chandra* orbit are comprised of orbital events and spacecraft commands that describe the telescope's position in space and commanding at a given time. These orbital elements and commands are given mnemonics to identify them. The mnemonics directly related to this analysis include OORMPDS (Radiation Monitor Disable), as well as EE1RADZ0 (AE-8 predicted radiation zone entry, for trapped electrons more energetic than 0.5 MeV), EPERIGEE (Perigee), XE1RADZ0 (AE-8 predicted radiation zone exit), and OORMPEN (Radiation Monitor Enable).

On a typical orbit, *Chandra's* radiation monitor process (called RADMON) will be disabled 10 ks prior to the AE-8 predicted electron 1 radiation zone entry. Because of the unpredictable nature of the radiation belts on entry and exit, disabling the RADMON prevents an autonomous radiation safing procedure from occurring. RADMON would of course trip on every belt passage if left enabled. At the same time as RADMON disable, ACIS translates out of the telescope's focus to shield the CCDs from low energy (100-200 keV) protons trapped in the radiation belts. Perigee passage follows after the AE-8 predicted entry and the AE-8 predicted electron 1 radiation zone exit soon follows that. The command to re-enable RADMON is typically executed 10 ks after the AE-8 predicted exit.

Figure 1 is a sample "light curve" showing the EPHIN P4 channel plotted along with CRM V2.3 flux for the month of October 2000, with perigee and radiation zone commanding overplotted. The "lower" data points correspond to the EPHIN P4 channel, while the "upper" data points correspond to the CRM V2.3 flux data during this time period. Also plotted on the secondary Y-axis is the CRM determined *Chandra* region: reg=3 denotes the magnetosphere; reg=2, the magnetosheath; and reg=1, the solar wind. Also noted in this example plot is an autonomus radiation safing procedure (known as "SCS 107") where the EPHIN P4 flux exceeded its limit of 300 $counts/sec/cm^2/sr$. Perigee is indicated by a vertical line, with RADMON disable/enable, and AE-8 predicted entry/exit orbital events surrounding perigee for each orbit.

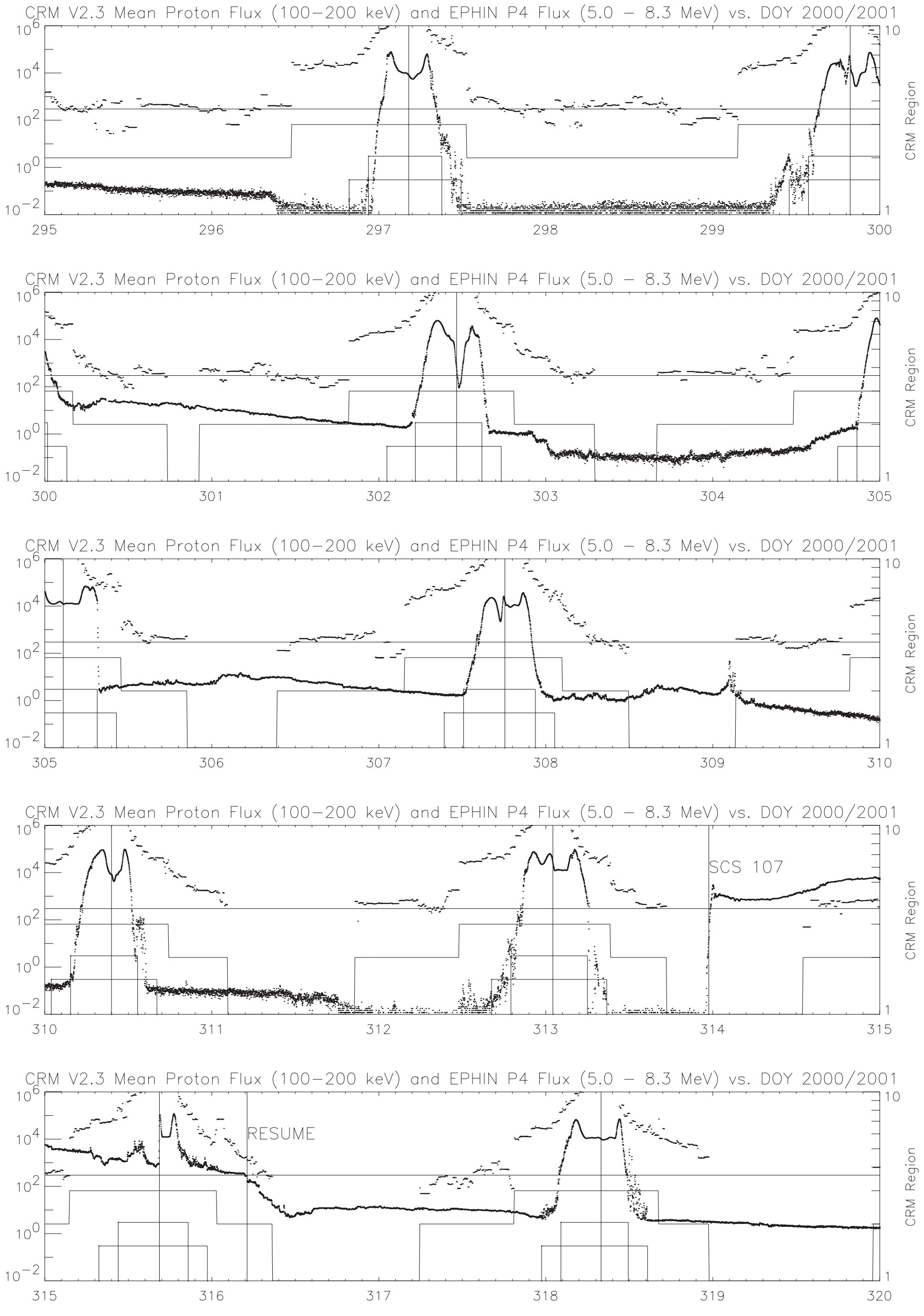

Figure 1.

EPHIN P4 and CRM V2.3 mean proton flux data vs time from Oct 21, 2000 (DOY 295) to Nov 15, 2000 (DOY 320). Please note that EPHIN and CRM are in different units: EPHIN is p/(cm^2 s sr) while CRM is p/(cm^2 s sr MeV). Plotted on the secondary y-axis is the CRM region. Horizontal lines correspond to the P4 SCS 107 limit, duration of RADMON disable, and duration of E1 entry. Note also the demarcation of an SCS107 autonomous radiation safing event; the start and end times of this particular event are noted on the plot.

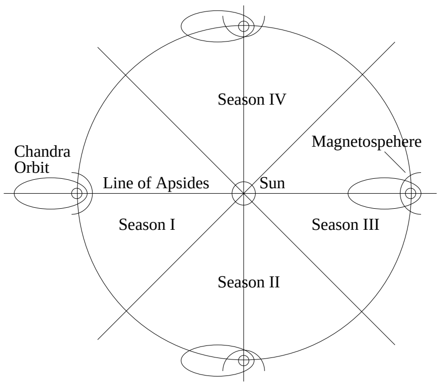

Figure 2. In season I *Chandra's* line of apsides is aligned with the RA of the Sun. This defines that season's midpoint and line drawn 45 degrees from either side of this point is the 90 day season. Notice that in season I all of *Chandra's* orbit is contained within the Earth's magnetosphere and in season III, most of the orbit is exposed to the solar wind. This is what drives the seasonal behavior that is seen in the data.

Table 1. Chandra Seasonal Midpoints

Dec Year
2000.0079
2000.9959
2001.9825
2002.9652

For the purpose of extracting the times of perigee passage per orbit, a database for all 5 of these events and their associated times for each orbit in the study was generated from the *Chandra* load review archive. Orbits in which *Chandra* was shut down either autonomously or manually due to high solar radiation events are not included in this analysis if *Chandra* was shut down through a perigee transit.

2.2. METHODOLOGY

In order to perform properly this analysis, *Chandra's* orbit must be categorized into seasons based on some phenomenological criterion. It was determined that the time of year when the right ascension of *Chandra's* line of apsides, the line connecting apogee and perigee, is equal to the right ascension of the Sun should be the defining seasonal characteristic. In this seasonal context, *Chandra's* orbit samples different space environments on a season by season basis (Fig. 2). The time of year for this orientation of the orbit was then found and the *Chandra* year was then broken down into 4 equal time intervals, where 1 in 4 intervals is centered on the dates in Table 1. Note that the *Chandra* year is slightly less than a sidereal because of the precession of its orbit.

Using these midpoints, the available data were divided into the 13 90-day quarters listed in Table 2. Each quarter was analyzed individually using the EPHIN P4 and E1300 and the CRM V2.3 data sets in conjunction with the database of orbital events focusing on the exact times of ingress and egress for each orbit. Using IDL, scatter plots were then generated depicting the CRM 100 keV to 200 keV proton fluxes against the EPHIN P4 and E1300 channels for ingress and egress. Here, the interval between OORMPDS and EE1RADZ0 defines ingress and that between XE1RADZ0 and OORMPEN, egress. As a starting point for comparison, a static *GLB* of 2.0E4 p/(cm^2 s sr MeV) was used throughout the initial analysis.

Table 2. Quarters Based on Seasonal Midpoints

Quarter	Year	Dates	DOY	DOY(1999)
IV	1999-2000	NOV28-FEB17	332-048	332-413
I	2000	FEB18-MAY17	049-138	414-503
II	2000	MAY18-AUG15	139-228	504-593
III	2000	AUG16-NOV14	229-319	594-684
IV	2000-2001	NOV15-FEB13	320-044	685-775
I	2001	FEB14-MAY15	045-135	776-867
II	2001	MAY16-AUG14	136-226	868-958
III	2001	AUG15-NOV13	227-317	959-1049
IV	2001-2002	NOV14-FEB12	318-043	1050-1139
I	2002	FEB13-MAY14	044-134	1140-1230
II	2002	MAY15-AUG13	135-225	1231-1321
III	2002	AUG14-NOV12	226-316	1322-1412
IV	2002-2003	NOV13-FEB11	317-042	1413-1503

Table 3. Quarter Midpoints and GLB values

Quarter	Mid (DOY 1999)	P4-IGLB	E1300-IGLB	P4-EGLB	E1300-EGLB
IV	373	2.8E4	4.5E4	2.2E4	2.3E4
I	459	1.0E5	1.1E5	NA	NA
II	549	1.1E5	NA	NA	NA
III	639	5.9E4	NA	4.9E4	9.9E4
IV	730	1.5E5	NA	1.1E4	8.9E3
I	821	4.6E4	NA	9.8E4	2.5E4
II	913	1.3E4	NA	2.9E5	NA
III	1004	2.1E4	3.7E4	7.7E4	NA
IV	1095	6.0E5	NA	NA	NA
I	1185	2.2E4	NA	NA	NA
II	1276	3.4E4	NA	4.5E5	NA
III	1367	2.6E4	2.6E4	8.9E3	5.4E4
IV	1458	NA	NA	NA	NA

3. RESULTS

3.1. CRM/EPHIN P4 SCATTER PLOTS

The scatter plots generated for each quarter on ingress and egress show the correlation, or lack thereof, between the EPHIN P4 and E1300 channels and the CRM database for the time frame of interest. The variable *GLB* for each plot is defined as the minimum CRM data point above the EPHIN P4 SCS107 threshold, currently set at 300 counts/sec/cm^2/sr. For the EPHIN E1300 channel, this limit is 10 counts/sec/cm^2/sr; however, the majority of quarters are dominated by the P4 channel results. The results of this *GLB* exploration per quarter are tabulated in Table 3. Entries marked with *NA* are a result of scatter plots in which there were no data points above the SCS 107 threshold for either one or both EPHIN channels. The column heading *IGLB* denotes the ingress *GLB*; *EGLB*, the egress *GLB*.

Figures 3 through 6 show the EPHIN P4 vs CRM scatter plots for all quarters on ingress and egress. In each panel, the initial constant *GLB* of 2.0E4 p/(cm^2 s sr MeV) is plotted along with the variable *GLB* found in each quarter. Also indicated in the lower left of each plot is the linear Pearson correlation coefficient between the EPHIN P4 and CRM data, and the exact value of the variable *GLB* for that plot. Notice that for all of these plots, this coefficient is very small, further indicating the lack of a correlation.

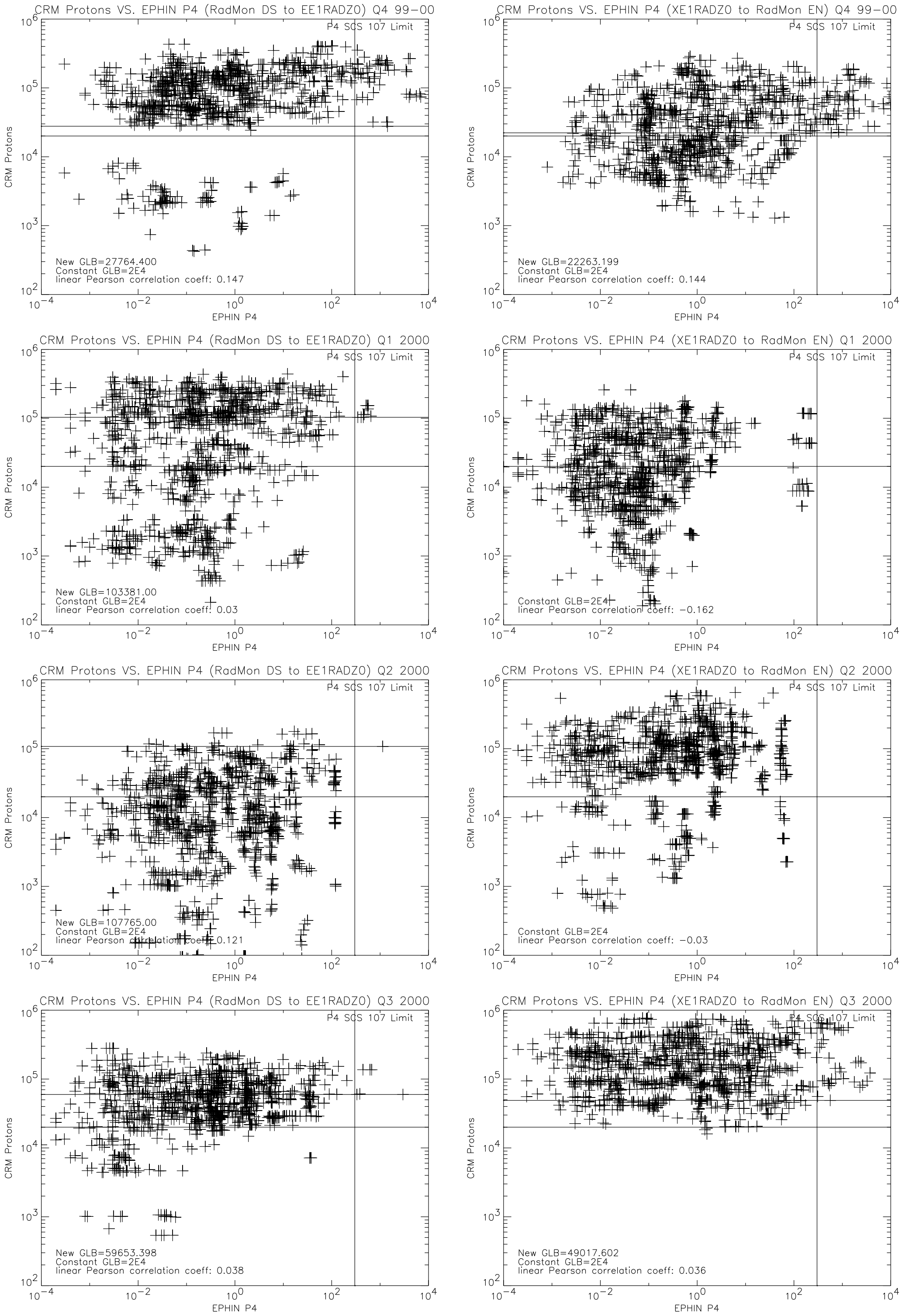

Figure 3. EPHIN P4 vs CRM scatter plots on ingress (left) and egress (right) from quarter 4 1999-2000 to quarter 3 2000.

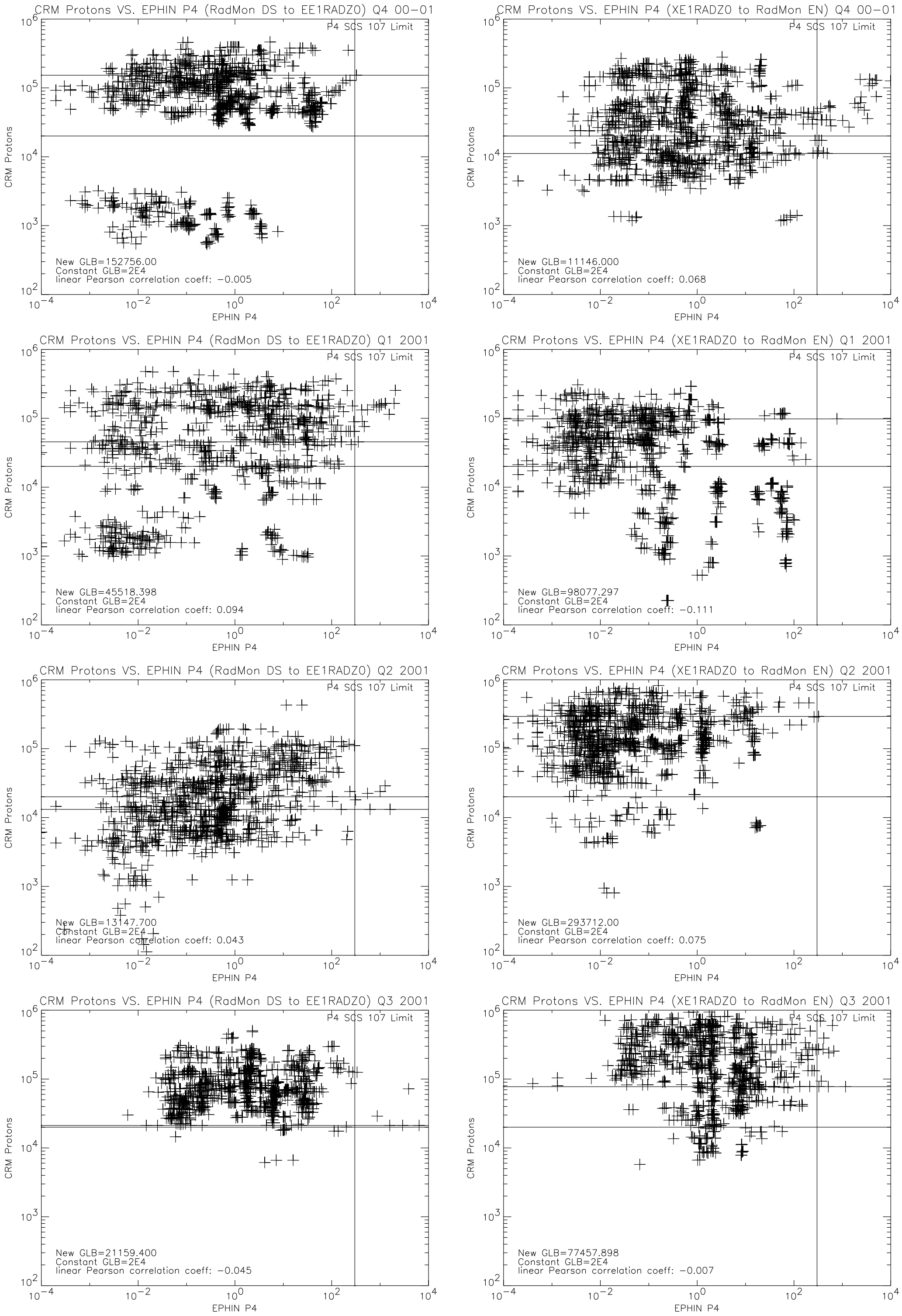

Figure 4. EPHIN P4 vs CRM scatter plots on ingress (left) and egress (right) from quarter 4 2000-2001 to quarter 3 2001.

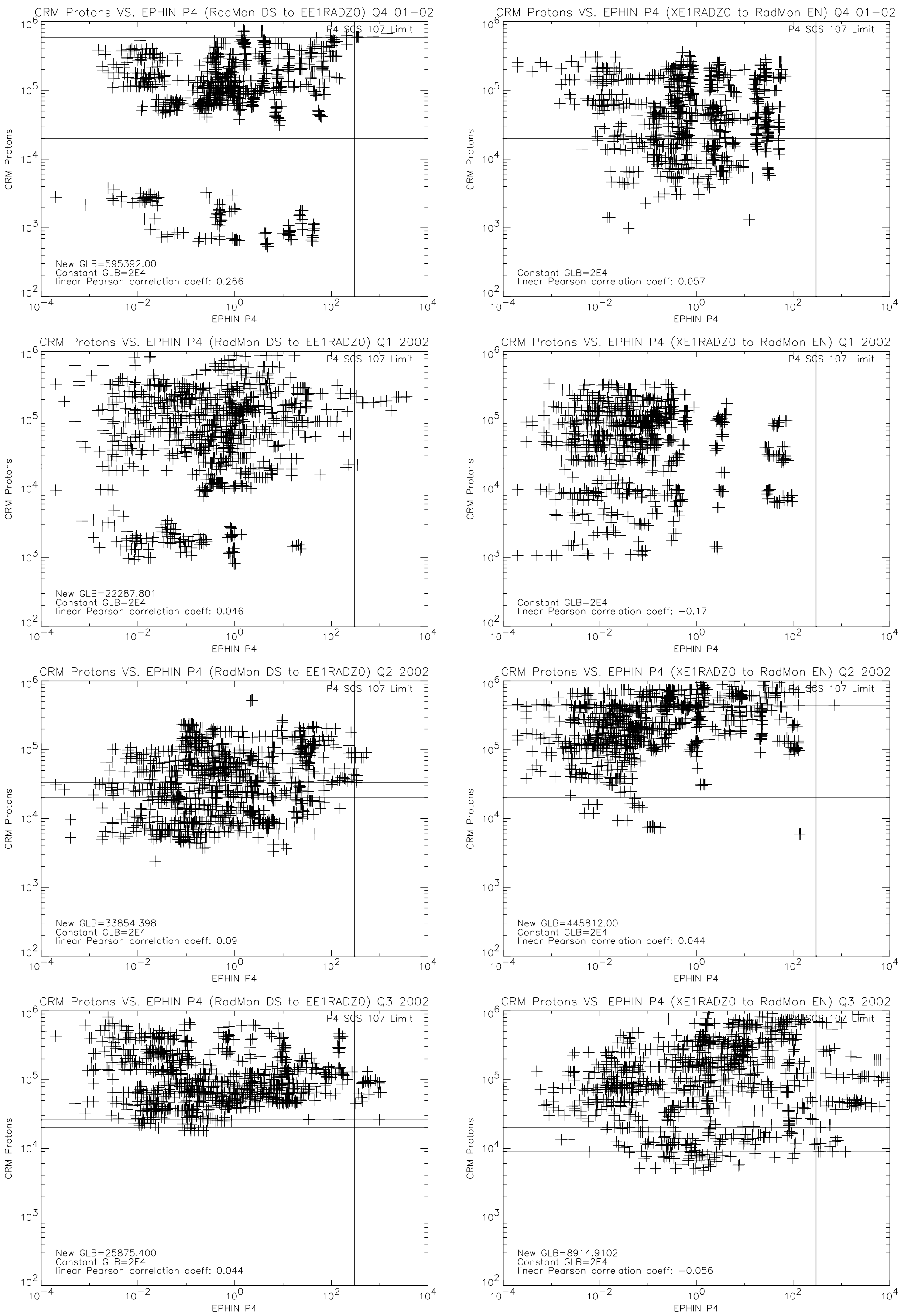

Figure 5. EPHIN P4 vs CRM scatter plots on ingress (left) and egress (right) from quarter 4 2001-2002 to quarter 3 2002.

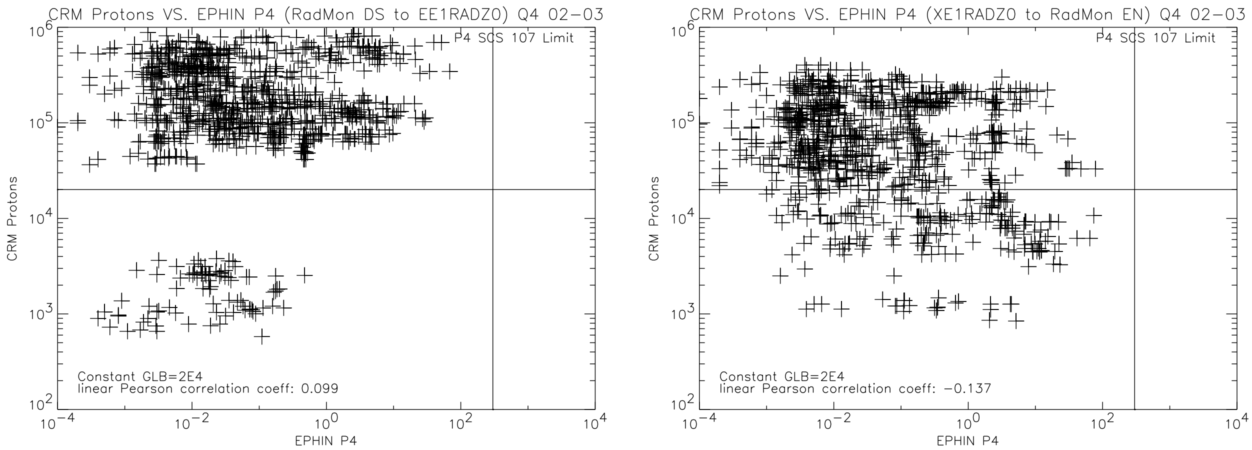

Figure 6. EPHIN P4 vs CRM scatter plots on ingress (left) and egress (right) from quarter 4 2002-2003.

3.2. Recovered Science Time & Seasonal Patterns

As a baseline starting point, the study incorporated a static *GLB* of 2.0E4 p/(cm^2 s sr MeV); any *GLB* found below that point in a quarter would have yielded one or more SCS107 trips. The initial constant-*GLB* analysis shows that there would have been 5 additional autonomous radiation safings (SCS107) — 1 on ingress and 4 on egress — had the *GLB* of 2.0E4 p/(cm^2 s sr MeV) been used since launch. Additionally, there would have been 1.8 Ms of recovered science time taken from the current 20 ks of pad time per orbit. This number of possible trips was considered unacceptable; hence, a new constant *GLB* of 0.8E4 p/(cm^2 s sr MeV), the minimum *GLB* found in 3.25 years of analysis, was evaluated. This reduced the amount of radiation trips to zero but also significantly reduced the recovered science time to 939 ks. It quickly became apparent that a more robust, varying *GLB* scheme might yield a higher science time recovery while minimizing radiation trips.

The third method of *GLB* driven science time recovery included the seasonal variations seen in the quarterly analysis. Figure 7 shows the *GLB's* listed in Table 3 versus time. Although there are limited statistics in this selection of data, in the 3.25 years analyzed there seems to be a pattern to the *GLB* vs time plot. Both the ingress and egress *GLB's* exhibit a sinusoidal behavior over time. It is worth noting that the egress points in quarters I and II in 2000 are actually unconstrained and were placed at 1.0E5 for plotting purposes. These points are most likely consistent with the other egress peaks found in 2001 and 2002. It is also worth noting that, with the exception of the first 3 quarters, the peaks in the egress *GLB's* are spaced apart by 6 months from the peaks of the ingress *GLB's.* This is directly related to the orientation of *Chandra's* orbit with respect to the Earth's radiation belts at that particular time of year. Naturally, *Chandra's* orbit samples a wide range of space environments throughout the year and in quarter IV *Chandra's* egress from perigee passes directly through an enhanced proton region, as reflected by the low egress *GLB's* in quarter IV. As the year progresses, this gradually changes such that *Chandra's* ingress towards perigee eventually samples this enhanced region, as evidenced by the low ingress *GLB's* in quarter II.

Table 4. Seasonal *GLB* Values

Quarter	IGLB	EGLB
I	2.0E4	2.0E4
II	1.0E4	2.0E4
III	2.0E4	8.0E3
IV	2.0E4	8.0E3

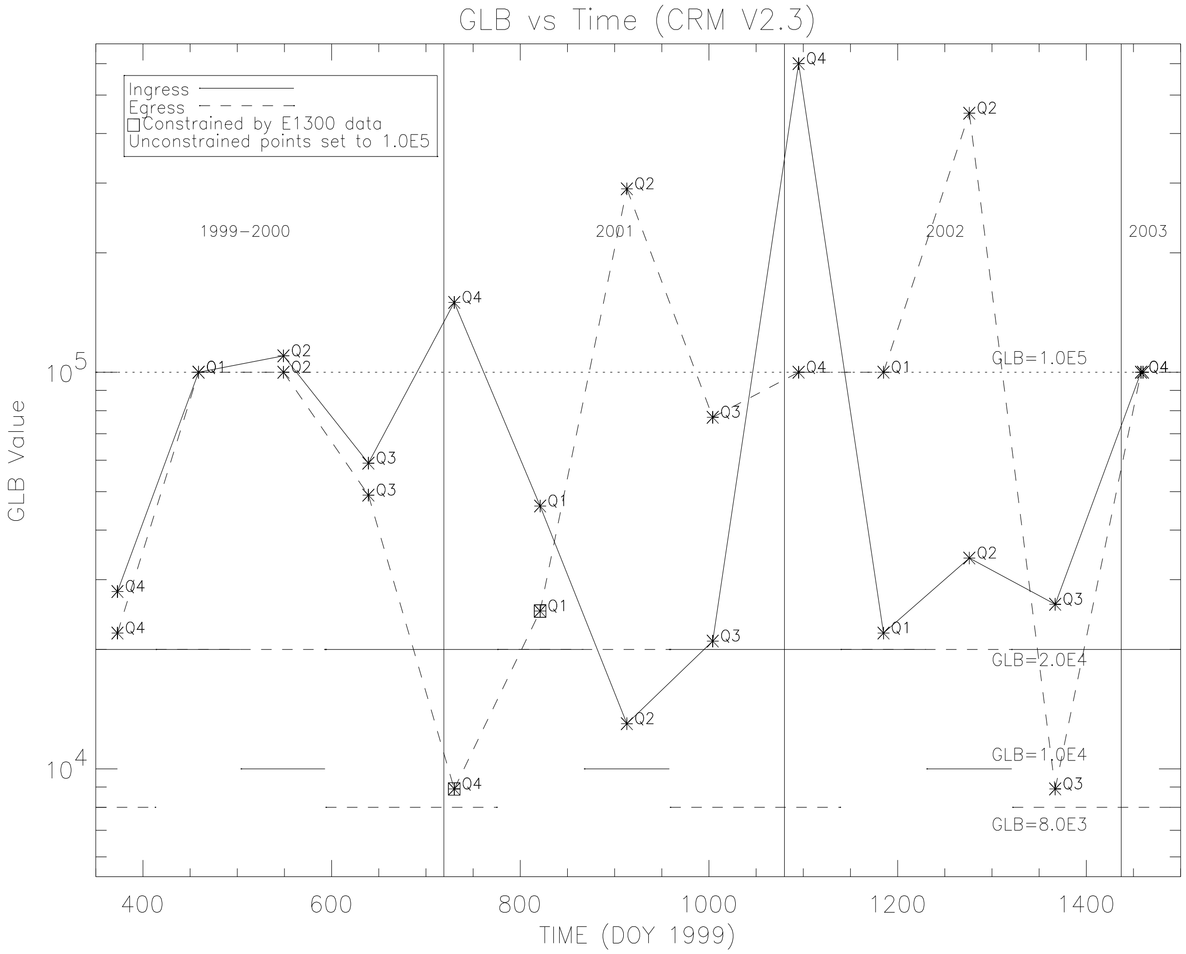

Figure 7. *GLB* vs Time from 28 November 1999 to 11 February 2003 using CRM V2.3. The *GLB* is taken directly from the scatter plots on ingress and egress and plotted at the midpoint of a quarter. Data points that are completely unconstrained are set to 1.0E5 p/(cm^2 s sr MeV). This CRM V2.3 seasonal *GLB* scheme yields a significant amount of recovered science time, with a minimal increase in radiation. Squares denote *GLBs* driven by E1300; all others are driven by P4. The seasonal *GLB*'s listed in Table 4 of this memo are plotted along the bottom of this graph as solid (ingress) and dashed (egress) lines.

Using the seasonal *GLB's* listed in Table 4 there would have been no autonomous radiation shut downs and the amount of recovered science time would total 1.35 Ms. The average amount of recovered science time per quarter on ingress would be 2.88 ks or the equivalent of one short observation. On egress, this average is slightly less at 1.88 ks, still a useful amount of recovered time. Table 5 gives a complete listing of the recovered science time and predicted CRM/P4 fluence per quarter.

The most effective use of *GLB's* it seems, would be to use a hybrid *GLB* scheme consisting of a constant *GLB* of 2.0E4 p/(cm^2 s sr MeV) on perigee ingress and the variable egress *GLB's* listed in Table 4. In this scenario, the study indicates that there would have been one SCS107 autonomous radiation shutdown in the 3.25 years studied. However, this shutdown would have occurred on ingress and there would have been sufficient time to recover and resume operations before exiting from perigee, thus not losing any additional science time. Using this *GLB* scheme, the total regained science time in 3.25 years is increased to 1373.98 ks, an increase

Table 5. Recovered Sci Time & Fluence per Quarter using CRM V2.3 Seasonal *GLB's*

Q	ITIME(ks)	ETIME(ks)	AvgI	AvgE	I-CRM-FLU	E-CRM-FLU	I-P4-FLU	E-P4-FLU
IV	32.60	30.90	2.17	1.34	2.13E8	1.53E8	1.34E4	4.03E3
I	86.07	174.06	2.69	5.62	4.89E8	1.49E9	2.56E4	2.03E5
II	188.06	30.69	6.07	2.05	1.16E9	2.58E8	3.02E5	4.36E4
III	30.42	0.00	2.54	0.00	2.34E8	0.00	9.64E3	0.00
IV	60.22	31.31	2.87	1.16	3.49E8	1.45E8	9.64E3	6.22E4
I	83.71	82.56	2.87	3.93	5.10E8	5.99E8	7.06E4	4.02E5
II	144.31	14.35	4.98	1.79	1.19E9	1.88E8	2.66E5	1.78E4
III	1.09	1.30	0.36	0.26	1.63E7	7.21E6	2.79E4	1.54E3
IV	45.21	26.92	2.83	1.22	2.84E8	1.48E8	1.05E5	3.71E4
I	62.81	62.63	2.99	3.13	4.43E8	4.60E8	3.34E4	1.31E5
II	87.58	10.01	4.61	2.00	7.55E8	1.41E8	3.56E4	2.84E4
III	0.12	7.63	0.12	0.64	0.00	4.22E7	0.00	2.07E4
IV	33.49	23.52	2.39	1.24	2.26E8	1.19E8	3.85E2	3.01E4

TOTAL Recovered Sci Time - Ingress: 855.69 ks, Egress: 495.90 ks, Total: 1351.60 ks
TOTAL CRM Fluence: 9.62E9 p/(cm^2 sr MeV), TOTAL P4 Fluence: 1.88E6 p/(cm^2 sr)

of 22.38 ks over the purely seasonal *GLB* analysis. The additional radiation exposure would mean a minimal increase in the predicted CRM fluence from 9.62E9 to 9.89E9 p/(cm^2 sr MeV) and the P4 predicted fluence from 1.88E6 to 1.97E6 p/(cm^2 sr).

4. CONCLUSIONS

We have presented the use of a seasonally based, variable *GLB* scheme to regain lost science time due to *Chandra's* radiation belt transit every 2 2/3 days. We have found that there may be a seasonal dependence in the CRM flux values that is linked to the orientation of *Chandra's* orbit throughout the year. We have also found a hybrid *GLB* scheme with a constant ingress *GLB* and a seasonally varying egress *GLB* to be a more robust and effective means of optimizing observing efficiency over the initial studies using a fixed *GLB* while maintaining a minimal increase in radiation exposure. This method would have regained 1.37 Ms of science observing time in the period from 28 November 1999 to 11 February 2003.

ACKNOWLEDGMENTS

The authors would like to acknowledge the help and support of the *Chandra* community, particularly members of the Chandra X-ray Center (CXC) for their pertinent discussions and suggestions. The Chandra X-ray Center is operated for NASA by the Smithsonian Astrophysical Observatory under contract NAS8-39073.

REFERENCES

1. S. N. Virani, R. Müller-Mellin, P. P. Plucinsky, and Y. M. Butt, "The Chandra X-ray Observatory's Radiation Environment and the AP-8/AE-8 Model," in *X-Ray Optics, Instruments, and Missions III*, J. Trümper and B. Aschenbach, eds., *Proc. SPIE.* **4012**, p. 669-680, 2000.
2. S. N. Virani et. al., "Improving the Science Observing Efficiency of the Chandra X-ray Observatory via the Chandra Radiation Model," in *X-Ray and Gamma-Ray Instrumentation for Astronomy XIII*, K.A. Flanagan and O.H.W. Siegmund, eds., *Proc. SPIE* **this volume**, 2003.
3. R. A. Cameron et. al., "Shelter from the Storm: Protecting the Chandra X-ray Observatory from Radiation," in *Proc. ADASS XI* **281**, p. 132-135, 2002.
4. W. C. Blackwell, Jr, J. I. Minow, S. L. O'Dell, R. M. Suggs, D. A. Swartz, A. F. Tennant, S. N. Virani, and K. M. Warren, "Modelling the Chandra Space Environment," in *X-Ray and Gamma-Ray Instrumentation for Astro. XI*, K. A. Flanagan and O. H. W. Siegmund, eds., *Proc. SPIE.* **4110**, p. 111-122, 2000.